Journal of the European Ceramic Society **14** (1994) 463–471

Temperature-Stable Dielectric Materials in the System $BaTiO_3$–Nb_2O_5–Co_3O_4

D. F. K. Hennings & B. S. Schreinemacher

Philips GmbH Research Laboratories Aachen, P.O. Box 1980, 52021 Aachen, Germany

(Received 6 January 1994; revised version received 22 April 1994; accepted 24 May 1994)

Abstract

Incorporation of Nb and Co and formation of dielectric ceramics were studied in ceramics of the system $BaTiO_3$–Nb_2O_5–Co_3O_4. Temperature-stable dielectric materials of the specification 'X7R' were found, showing permittivities up to $K \cong 4800$.

The slow volume diffusion of Nb favours the formation of 'core-shell' structures in $BaTiO_3$ which are responsible for the temperature-stability. Pentavalent Nb and divalent Co show a pronounced co-solubility in $BaTiO_3$. At the atomic ratio Nb:Co = 2:1 semiconductive materials occur which show the PTCR effect. The ratio of Nb:Co = 2:1 strongly suggests charge compensation of $[Nb^{5+}]$-donors by $[Co^{2+}]$"-acceptors on Ti sites, forming the complex $[Nb^{5+}_{2/3}Co^{2+}_{1/3}]^{4+}$.

The insulation resistance and life stability of thin dielectric layers of $BaTiO_3$–Nb,Co X7R material are determined by the interconnection of lower insulating undoped $BaTiO_3$ cores. The percolation limit depends on the dispersal of Nb_2O_5 and Co_3O_4 over the $BaTiO_3$.

Der Einbau von Nb und Co und die Bildung temperaturstabiler dielektrischer Keramiken wurden in Keramiken des Systems $BaTiO_3$–Nb_2O_5–Co_3O_4 untersucht. Temperaturstabile Materialien der Spezifikation 'X7R' mit Dielektrizitätskonstanten bis zu $\varepsilon_r \cong 4800$ wurden gefunden.

Die geringe Volumendiffusion von Nb und Co begünstigt die Entstehung von 'core–shell'-Strukturen und ist eine wichtige Voraussetzung fur die Bildung temperaturstabiler Materialien. Nb und Co zeigen eine ausgeprägte Konsolubilität auf den Titanplätzen des Perowskitgitters. In der Nähe des atomaren Verhältnisses Nb:Co $\cong$ 2:1 treten halbleitende Keramiken auf, die den PTCR-Effekt zeigen. Das atomare Verhältnis von Nb:Co = 2:1 legt nahe, daß Ladungskompensation von $[Nb^{5+}]$-Donatoren und $[Co^{2+}]$"-Akzeptoren auf den Ti-Plätzen des Perovskitgitters stattfindet.

Der Isolationswiderstand und die Lebensdauer von dünnen dielektrischen Schichten werden maßgeblich durch die Perkolation der $BaTiO_3$-cores bestimmt, die eine höhere ionische Leitfähigkeit aufweisen als das dotierte Material.

L'incorporation de Nb et Co et la formation de céramiques diélectriques ont été étudiées dans le système $BaTiO_3$–Nb_2O_5–Co_3O_4. Un matériau diélectrique stable en température de spécification 'X7R' a été mis au point avec une permittivité $K \approx 4800$. La faible diffusion en volume de Nb favorise la formation d'une structure 'core-shell' dans $BaTiO_3$, laquelle est responsable de la stabilite en température. Le Nb pentavalent et le Co divalent montrent une co-solubilité prononcée dans $BaTiO_3$. Un matériau semi-conducteur apparait pour un raport atomique Nb:Co = 2:1 montrant l'effet PTCR. Ce rapport Nb:Co = 2:1 suggère fortement un effet de compensation de charge des $[Nb^{5+}]$-donneurs par $[Co^{2+}]$"-accepteurs sur les sites Ti, formant le complexe $[Nb^{5+}_{2/3}Co^{2+}_{1/3}]^{4+}$. La résistance d'isolation et la stabilité de couches minces diélectriques de matériaux $BaTiO_3$–Nb, Co X7R sont déterminées par interconnexion de coeurs en $BaTiO_3$ non dopés et de faible effet isolant. La limite de percolation dépend de la dispersion de Nb_2O_5 et Co_3O_4 dans $BaTiO_3$.

1 Introduction

1.1 Temperature-stable (X7R) dielectrics

For the manufacture of ceramic multilayer capacitors (MLCs) various dielectric materials are employed, showing different permittivities, loss factors and temperature coefficients (TCC) of the permittivity. Some of the most desired materials are the temperature-stable dielectrics of the EIA (Electronic Industries Association specification) 'X7R'. The dielectric temperature specification X7R allows maximum deviations of the capacitance of ±15%

Journal of the European Ceramic Society 0955-2219/94/$7.00

from the 20°C reading within the temperature range −55°C to +125°C

Even today the composition of most dielectric ceramics is based on ferroelectric $BaTiO_3$. Pure $BaTiO_3$ and homogeneous mixed crystals of $BaTiO_3$, however, are usually not able to meet the stringent regulations of the specification X7R. The temperature stability of X7R materials is the result of a very fine chemical heterogeneity of the material. In a first approach X7R materials can be treated as a fine-grained mixture of pure $BaTiO_3$ and a second ferroelectric phase, having the dielectric Curie maximum at the low temperature end[1] of the specification X7R. In transmission electron microscopy (TEM) X7R materials often exhibit so-called 'core-shell' structures. Core-shell materials have a strong chemical heterogeneity within the grains. The grain cores consist of practically pure ferroelectric $BaTiO_3$, whereas the shell region is heavily doped.[2,3] The grain shell is, in contrast to the core, paraelectric at room temperature. Core-shell materials are generally rather unstable and sensitive to firing conditions. Due to their heterogeneous structure they have a strong trend to homogenize and to form mixed crystals. Reproduction of the flat dielectric temperature characteristics of X7R materials therefore needs careful control of the mixing and firing conditions.

1.2 The system $BaTiO_3$–Nb_2O_5–Co_3O_4

X7R materials of the system $BaTiO_3$–Nb_2O_5–Co_3O_4 are well known for their high permittivity values of $K \cong 3000$–5000. Moreover, dielectric powders of this system are relatively easy to handle compared to other X7R formulations. $BaTiO_3$–Nb, Co materials are therefore preferentially employed for the manufacture of multilayer capacitors. The high insulation resistance (IR) makes these materials also promising candidates for use in thin dielectric layers.

The permittivity level of $BaTiO_3$–Nb,Co X7R materials critically depends on the grain size of the $BaTiO_3$ which is optimum at 0·6–0·9 μm.[4,5] The temperature characteristic of X7R materials is determined by the degree of micro-heterogeneity at the distribution of Nb and Co over $BaTiO_3$. Too fine mixing leads to formation of homogeneous mixed crystals and a loss of temperature stability.

Additives of niobium pentoxide are known to lower the Curie point of $BaTiO_3$ and to form broad, diffuse dielectric maxima.[6] Kahn & Buessem[7] detected Nb-enriched grain boundaries in Nb-doped $BaTiO_3$. The broad diffuse dielectric maxima at the Curie points of these materials were interpreted as a result of inhomogeneous distribution of Nb. Burn[8] observed easy regulation of the Nb distribution over $BaTiO_3$ by addition of small amounts of CoO, MgO or NiO. Nowadays, X7R materials with Co_3O_4 additives are preferentially used for the manufacture of MLCs.

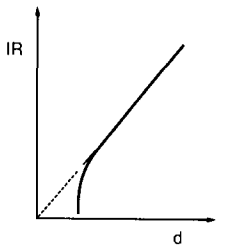

Fig. 1. Correlation (schematical) between insulation resistance (IR) and thickness (d) of a dielectric layer in conventional $BaTiO_3$–Nb_2O_5–Co_3O_4 X7R material.

1.3 Thin dielectric layers of $BaTiO_3$–Nb_2O_5–Co_3O_4

In the field of passive components the continuous trend of miniaturization leads to smaller and smaller MLCs with thin dielectric layers being less than 10 μm. For thin dielectric layers highly insulating ceramics are needed which must have a high endurance under strong electrical field and temperature stress. A serious problem with thin layers of the $BaTiO_3$–Nb,Co X7R material, however, is the trend to electrical degradation and lowered resistance even under low DC field stress. Figure 1 schematically illustrates the correlation between insulation resistance and thickness of the dielectric layer. For a given electric field the specific resistance of a thin dielectric layer is much lower than that of a thicker layer having the same nominal composition. Corresponding to the internal heterogeneity of the dielectric ceramic, certain small regions of lower resistive material are assumed to extend from one electrode to the other in thin dielectric layers.

1.4 Aim of the investigation

Insulation resistance, life stability and TCC of $BaTiO_3$–Nb,Co X7R materials obviously critically depend on the micro-distribution of Nb and Co within the $BaTiO_3$. This paper deals with the relations between micro-heterogeneity and insulation resistance of thin dielectric layers of $BaTiO_3$–Nb, Co X7R materials, incorporation and diffusion of Nb and Co, the valency state of Co and the defect chemistry of both additives.

2 Experimental

2.1 Raw materials used

For preparation of dense ceramic materials fine, reactive powders of $BaTiO_3$ have to be employed. Fine powders of pure $BaTiO_3$ were obtained either from calcined barium titanyl oxalate (BTO) or by

hydrothermal synthesis. The BTO-based barium titanate[9] (TAM Ceramics, Inc., Niagara Falls, USA) had a particle size of d_{50} = 0·9 μm and a crystallite size of ≅0·3 μm, while the hydrothermal $BaTiO_3$[10] (Cabot Corporation, Boyertown, PA, USA) had an average particle size of d_{50} = 0·4 μm and a crystallite size of ≤0·1 μm. Using X-ray fluorescence (XFA), the atomic ratios of Ba and Ti of the $BaTiO_3$ powders used were determined to lie in the range 1·002 < Ti/Ba < 1·006. Reagent grade Nb_2O_5 (H. C. Starck, Goslar, Germany) and Co_3O_4 (PA, Merck, Darmstadt, Germany) were intensively ball-milled to particle sizes of $d_{50} \leq 0{\cdot}3$ μm, using *Y*-stabilized ZrO_2 balls.

2.2 Preparation of ceramic disc capacitors (CDCs)

Hydrothermal and BTO-based $BaTiO_3$ were wet mixed with Nb_2O_5 and Co_3O_4 in various concentrations up to 5 at.% Nb and 2 at.% Co, using an agate ball mill. The mixed powders were dried and uniaxially pressed at 3·3 kbar to ceramic discs of 5 mm diameter and 0·6 mm thickness. The discs were fired in air at temperatures in the range of 1200 to 1500°C. Hydrothermal powders became dense at *c.* 1250°C, while BTO-based powders needed temperatures of *c.* 1300°C for densification. Ceramic disc capacitors (CDC) were prepared by evaporating Cr/Ni-Au electrodes on the discs.

Permittivity and dielectric losses were measured at 1 kHz and 1 Vrms in the temperature range −60°C to +150°C. The dielectric strength was determined on CDCs by measuring the DC field dependence of the specific resistance, σ. Ferroelectric polarization currents distorting the measurement of σ were largely suppressed by heating the samples above the Curie point. By increasing the DC field in small steps and waiting about 5 time constants (5 · R · C) for each measuring point, the measured sample currents appeared fairly time-stable.

For STEM investigations CDCs were mechanically lapped and polished to about 15 μm and thereafter ion-beam etched to <50 nm thickness.

2.3 Preparation of diffusion couples

A suitable way to study solid-state reactions between $BaTiO_3$, Nb_2O_5 and Co_3O_4 is firing of diffusion couples of the reactants at various temperatures. Diffusion couples were produced from 50 μm thick ceramic foils of $BaTiO_3$, Nb_2O_5 and mixtures of Nb_2O_5 + Co_3O_4 (Nb : Co = 2·5 : 1). Using the doctor-blade technique, the foils were tape-cast from aqueous suspensions of ceramic powder and polyvinyl alcohol (PVA) binder.

The green foils were stacked and pressed to 'sandwiches', consisting of cover layers of 500 μm $BaTiO_3$ (10 foils of thickness 50 μm) and a central layer of 100 μm Nb_2O_5, or Nb_2O_5 + Co_3O_4 (2 foils of thickness 50 μm). After carefully burning out the organic binder at 525°C in air, the couples were heated at 4°C/min to temperatures of 1200°C to 1380°C and held for 1h. To prevent delamination of the couples, firing was performed under low mechanical pressure, using the weight of small alumina bars. The alumina weights were separated from the $BaTiO_3$ couples by thin Pt sheets. After firing, the concentration profiles of Nb, Co, Ba and Ti were determined on polished cross-sections of the couples by using electron microbeam techniques. Additional information about the phases formed during heating was obtained from X-ray diffraction (XRD) analyses of polished sections of the couples.

3 Results

3.1 Ceramic disc capacitors

In dense ceramics fired at 1300°C grain growth was rather poor with exception of those materials having a Nb : Co atomic ratio slightly below 2 : 1. At Nb : Co = 2 : 1 the materials recrystallized at T > 1270°C, yielding grains of >10 μm. All other materials had grain sizes of <1 μm. In samples fired above 1300°C long dendritic needles of Ti-rich second phase were observed. Dielectric results are shown in Fig. 2. The figure is divided into two sections by a line, denoting the atomic ratio Nb : Co = 2 : 1. In the lower section a number of interesting X7R materials was found, showing permittivities up to K = 4800. Materials of the upper section and those having compositions far below of the line Nb : Co = 2 : 1 exhibited broad dielectric maxima, falling outside the specification X7R. Recrystallized ceramics occurring just below the line Nb : Co = 2 : 1 were, in contrast to the other materials, semiconductive, showing a positive temperature characteristic of resistance (PTCR effect), see Fig. 3.

3.2 Reaction of Nb_2O_5 and Co_3O_4 with $BaTiO_3$

3.2.1 XRD and dielectric studies

Nb_2O_5 is known for its slow and incomplete reaction with $BaTiO_3$. Figure 4 shows minimal changes of the lattice parameters for samples of $BaTiO_3$–4Nb ($BaTiO_3$ + 0·02 Nb_2O_5) which were heated in the temperature range of 1200°C to 1450°C. Materials doped with Nb and Co (Nb : Co = 2·5 : 1) exhibited, in contrast distinct changes of the lattice parameters, indicating better incorporation in the case of combined doping. The TCC of Nb, Co-doped material (Fig. 5, curve (b)), fits well into

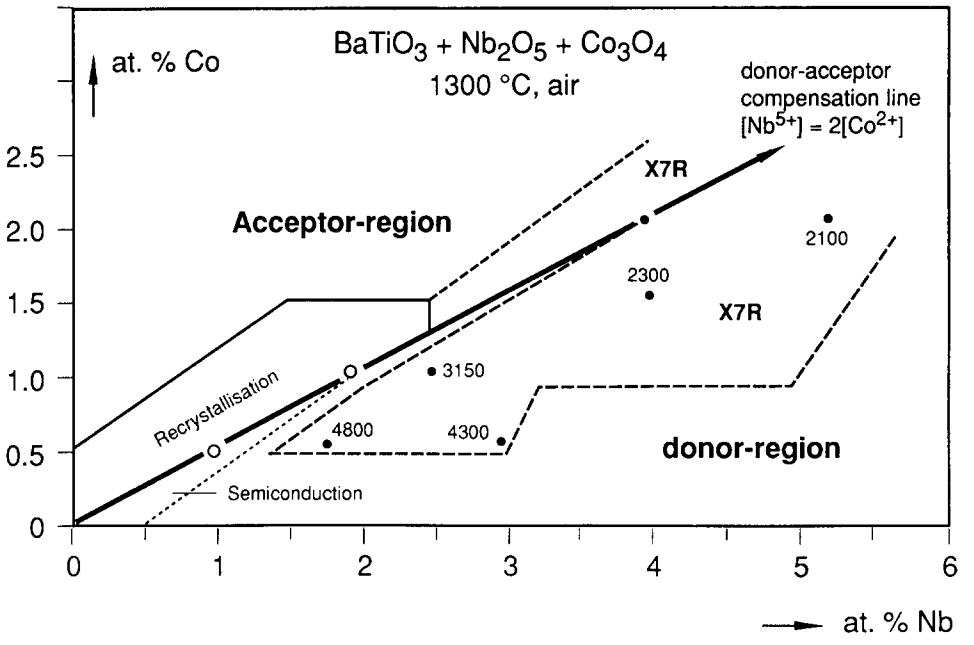

Fig. 2. Dielectric results, obtained in samples of the system $BaTiO_3$–Nb_2O_5–Co_3O_4, fired 2 h at 1300°C in air (conventional, oxalate-based $BaTiO_3$). ○, PTC semiconductive materials; ●, highly insulating dielectrics.

the specification X7R, while that of single Nb-doped material, (Fig. 5, curve (a)), is characterized by a broad and diffuse dielectric maximum.

3.2.2 Lattice site of Nb, valency state of Co

On the basis of ionic radii, the ions of Nb^{5+}, Co^{3+} and Co^{2+} are expected to enter the Ti-sites of $BaTiO_3$. Large amounts of Ti-rich phase formed during the sintering of $BaTiO_3$–Nb,Co materials strongly support the idea that Ti is replaced by Nb and Co. According to the phase diagram of Negas *et al.*[11], TiO_2 reacts with $BaTiO_3$ to form the Ti-rich phase $Ba_6Ti_{17}O_{40}$.

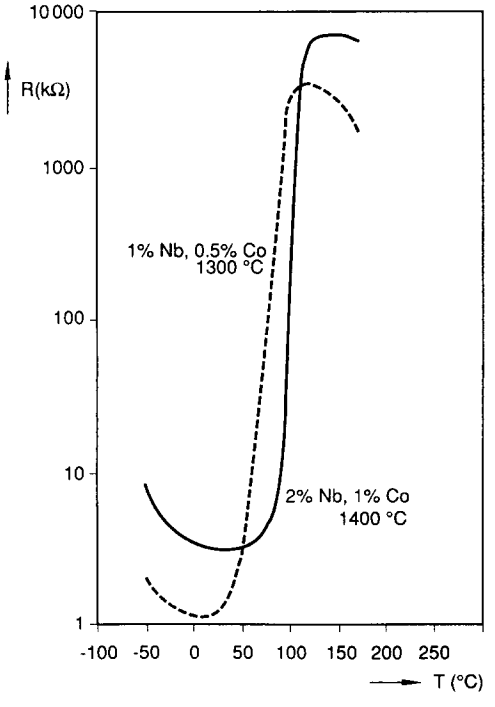

Fig. 3. Positive temperature characteristics of resistivity (PTCR effect), observed in samples, containing Nb and Co in the atomic ratio 2:1.

Pentavalent ions of Nb on Ti-sites are $[Nb_{(Ti)}]$ donors which are compensated by Ti-vacancies $[V_{(Ti)}'''']$ in an oxidizing atmosphere.[12,13] The ions of Co^{2+} and Co^{3+} on Ti-sites are in contrast acceptors, $[Co_{(Ti)}]''$ and $[Co_{(Ti)}]'$, which are compensated by oxygen vacancies $[V_O]''$.[14] In the case of the combined addition of Nb_2O_5 and Co_3O_4 the Nb-donors and Co-acceptors are expected to compensate each other. The occurrence of PTCR-type semiconductive materials at Nb : Co ≅ 2 : 1 strongly supports the idea that Nb^{5+}-donors are compensated by Co^{2+}-acceptors. The PTCR effect only appears at a small excess (<0·4 at.%) of donor doping[11] in $BaTiO_3$. In Fig. 2 the line denoting the ratio N : Co = 2 : 1 marks the boundary between net acceptor-doped (upper section) and net donor-doped materials (lower section). The complex perovskite compound $Ba(Nb^{5+}_{2/3}Co^{2+}_{1/3})O_3$ is in fact known from the literature.[15] The dielectric properties of $BaTiO_3$–Nb,Co materials are most probably

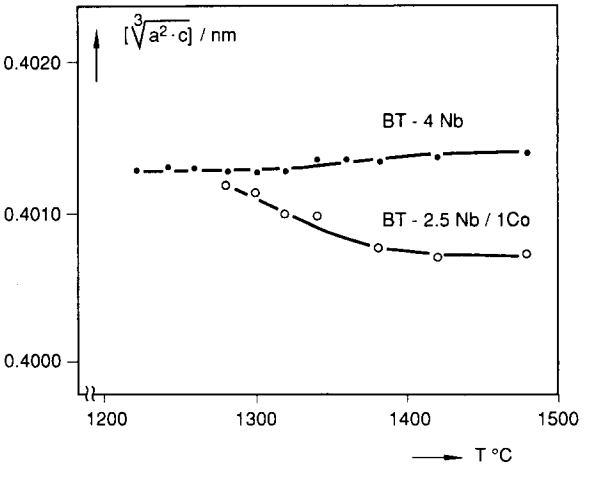

Fig. 4. Lattice parameters of $BaTiO_3$ with additions of ●, 0·02 mol Nb_2O_5 and ○, 0·0125 mol Nb_2O_5 + 0·0033 Co_3O_4, fired at temperatures of 1200°C to 1500°C in air.

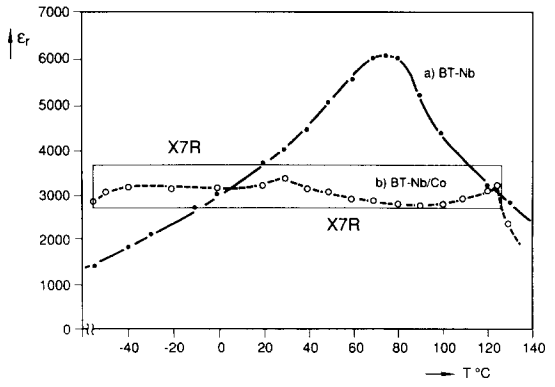

Fig. 5. Dielectric temperature characteristic of (a) $BaTiO_3$ + 0·015 Nb_2O_5, fired 2 h at 1450°C and (b) $BaTiO_3$ + 0·0125 Nb_2O_5 + 0·0033 Co_3O_4, fired 2 h at 1300°C.

significantly determined by the complex $[Nb^{5+}_{2/3}Co^{2+}_{1/3}]^{4+}$ substituting for Ti^{4+}.

3.2.3 Diffusion couples

In the system BaO–TiO_2–Nb_2O_5 a large number of ternary phases exist. Detailed investigations of the system $BaTiO_3$–Nb_2O_5 have been carried out by Roth and coworkers.[16–18] XRD data of some of these phases are available in the JCPDS powder diffraction file.[19] The XRD reflections of the following phases were detected in polished sections of diffusion couples of $BaTiO_3$–Nb_2O_5 which were heated for 1 h at 1250°C in air:

$BaTiO_3$	(Main phase)
$Ba_3Nb_{10}O_{28}$	(Weak)
$BaNb_2O_6$	(Strong)
$Ba_3Ti_5Nb_{3\cdot2}O_{21}$	(Weak)
$Ba_2Ti_5O_{12}$	(Weak)

In $BaTiO_3$–Nb_2O_5–Co_3O_4 couples, annealed for 1 h at 1250°C in air, $CoNb_2O_6$ additionally appeared. SEM micrographs of diffusion couples of $BaTiO_3$–Nb_2O_5 and $BaTiO_3$–Nb_2O_5–Co_3O_4, heated for 1 h at 1250°C in air, are shown in Fig. 6(a) and 6(b). Even in sintered couples the sequence of $BaTiO_3$ layers was still visible at the darkish lines where the green foils had been stacked together. Using these lines as simple markers, the direction of growth and diffusion of the phases formed during firing were determined. In SEM the material contrast clearly indicates layers of different phases. Quantitative microbeam analyses revealed the following phases formed at 1250°C in couples of $BaTiO_3$–Nb_2O_5.

Cover layer	$BaTiO_3$ (depletion of BaO),
Layer I	$Ba_2Ti_5O_{12}$ (with NbO dissolved)
Layer II	$Ba_3Ti_4Nb_4O_{21}$ (with $BaTiO_3$ dissolved)
Layer III	$BaNb_2O_6$ (with TiO_2 dissolved) $Ba_6Nb_{14}O_{38}$, $Ba_3Nb_{10}O_{28}$ (minor amounts)

Microanalyses of the couples revealed a high mobility of BaO already at 1250°C, as seen by the drift of BaO from the $BaTiO_3$ cover layers to the central Nb_2O_5 layer. The Nb_2O_5 layer was thus completely changed into $BaNb_2O_6$ (BN_2), $Ba_6Nb_{14}O_{38}$ (B_6N_{14}) and $Ba_3Nb_{10}O_{28}$ (B_3N_{10}). BN_2 and B_3N_{10} were detected by XRD. The sequence of phases observed in couples of $BaTiO_3$–Nb_2O_5 (Fig. 7) strongly suggests initial formation of BN_2 and $Ba_2Ti_5O_{12}$ (B_2T_5) at the contact of $BaTiO_3$ and Nb_2O_5. In a subsequent step B_2T_5 and BN_2 seem to form a layer of a ternary phase, having the atomic ratio Ba : Ti : Nb ≅ 3 : 4 : 4. The composition of this phase agrees well with the ternary compound $Ba_3Ti_4Nb_4O_{21}$ ($B_3T_4N_4$), reported by Mercey *et al.*[2] The microanalytical studies also confirmed the broad compositional range of $B_3T_4N_4$ with respect to variations of Ti and Nb. Roth and coworkers[16] derived for $B_3T_4N_4$ the general formula $Ba_3Ti_{4+5x}Nb_{4-4x}O_{21}$ ($0 \leq x \leq 0{\cdot}3$). These authors observed that this phase is in direct equilibrium with Nb-saturated $BaTiO_3$. $B_3T_4N_4$ is thus formed when the solubility limit of Nb in $BaTiO_3$ is exceeded. $Ba_2Ti_5O_{12}$ was first discovered by Jonker & Kwestroo.[13] Later its existence was questioned by Negas *et al.*[11] In agreement with Roth and coworkers,[16] however, it could be confirmed that $Ba_2Ti_5O_{12}$ is stabilized by small amounts of dissolved Nb_2O_5.

In diffusion couples of $BaTiO_3$–Nb_2O_5/Co_3O_4, fired for 1 h at 1250°C, (Fig. 7(b)), the central layer of Nb_2O_5/Co_3O_4 was completely changed to $CoNb_2O_6$. Even at 1250°C the $CoNb_2O_6$ did not dissolve considerable amounts of BaO or TiO_2. Between the layers of $BaTiO_3$ and $CoNb_2O_6$ a coherent layer of $BaNb_2O_6$ was found with appreciable amounts of Co dissolved. Small islands of $BaNb_2O_6$ were spread over the $CoNb_2O_6$. From this it may be deduced that BN_2 is in direct equilibrium with $BaTiO_3$ and $CoNb_2O_6$. The phase $B_3T_4N_4$, detected in couples of $BaTiO_3$–Nb_2O_5, was not observed in $BaTiO_3$–Nb_2O_5. In couples of $BaTiO_3$–Nb_2O_5, fired at 1250°C, the B_2T_5 had dissolved large amounts of Co. The large clusters of BN_2 and B_2T_5 scattered over the matrix of $BaTiO_3$ were already formed on heating at 1250°C. In the undoped system $BaTiO_3$–TiO_2 the Ti-rich phase $Ba_6Ti_{17}O_{40}$ forms a liquid eutectic with $BaTiO_3$ at 1312°C.[11] In Nb,Co-doped $BaTiO_3$ the eutectic temperature is lowered to about 1270°C. Distribution and incorporation of Nb_2O_5 and Co_3O_4 in $BaTiO_3$ are strongly accelerated by liquid phases, having Nb and Co dissolved.

3 TEM and STEM studies

The minimal change of lattice constants, observed in mixtures of $BaTiO_3$–Nb_2O_5 (Fig. 4) confirmed

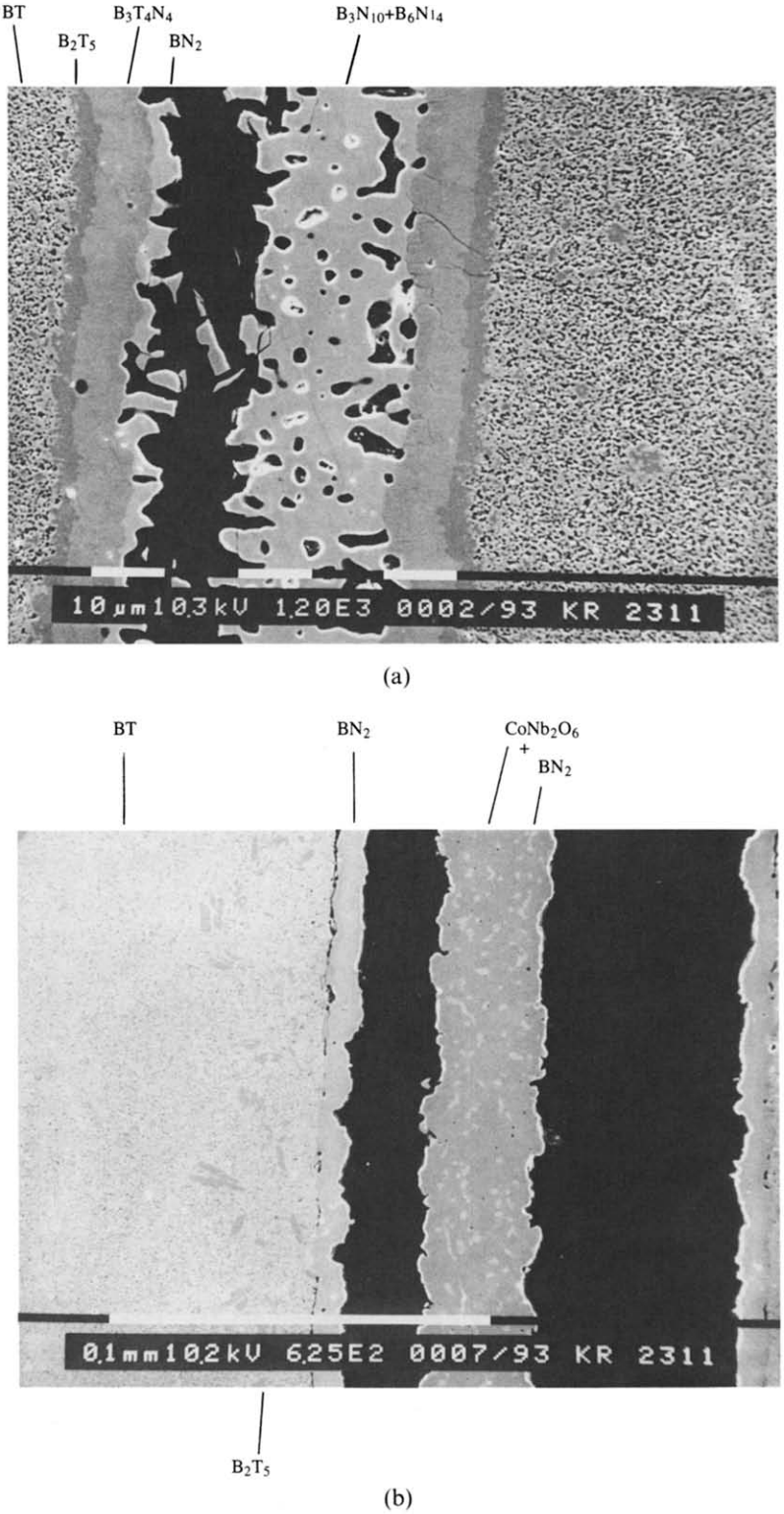

Fig. 6. SEM micrographs of diffusion couples: (a) $BaTiO_3$ (500 μm)–Nb_2O_5(100 μm)–$BaTiO_3$(500 μm), fired for 1 h at 1250°C; (b) $BaTiO_3$ (500 μm), Nb_2O_5/Co_3O_4 (100 μm, Nb/Co = 2·5 : 1)–$BaTiO_3$ (500 μm), fired for 1 h at 1250°C.

the poor homogenization of Nb in $BaTiO_3$. STEM inspection of ion-beam etched CDCs of $BaTiO_3$–Nb,Co X7R material (Fig. 8) revealed typical core-shell structures in the grains. The intragranular heterogeneity was also confirmed by EDAX analyses in STEM. Using a fine electron beam of <4 nm diameter, small relative changes of the Nb and Co concentration could be detected with a local resolution of <20 nm. The concentrations of Nb and Co are given in arbitrary units, based on the measured count rates of Nb-L_α and Co-K_α. Figure 8 shows the inhomogeneous distribution of Nb and Co along a line of spots (analysis numbers 1–6) in a grain of X7R material. The Nb and Co concentrations determined in spot numbers 10–12 agree well with those of numbers 1 and 2 (shell region). Core-shell regions were even found in samples heated up to 1350°C. The

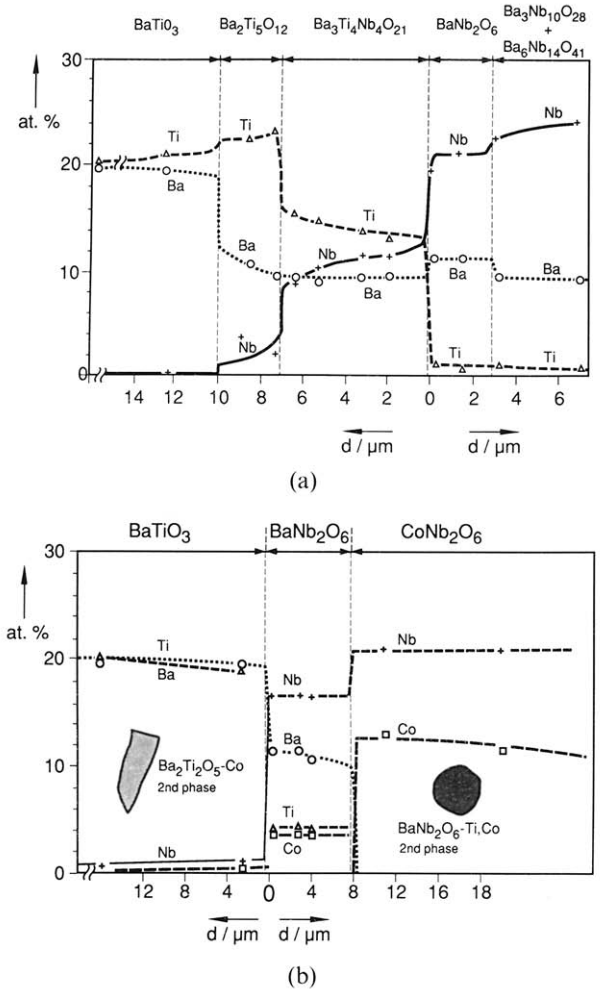

Fig. 7. EDAX analysis of atomic concentrations of Ba, Ti, Nb and Co, determined in diffusion couples: (a) $BaTiO_3$–Nb_2O_5–$BaTiO_3$, fired for 1 h at 1250°C; (b) $BaTiO_3$–NB_2O_5/Co_3O_4(Nb/Co = 2.5 : 1)–$BaTiO_3$, fired for 1 h at 1250°C.

narrow coexistence of poorly doped material in the grain cores and heavily doped material in the shells suggests extremely low volume diffusion coefficients of Nb and Co in $BaTiO_3$. The very slow diffusion of Nb and Co through the grains is considered as a fundamental prerequisite for the formation of temperature-stable X7R materials.

3.3.1 Co-solubility of Nb and Co

Although Nb_2O_5 and Co_3O_4 powder were separately added to $BaTiO_3$, the grain shells generally contained a combination of both elements in a ratio close to Nb : Co ≅ 2 : 1. Regions with high concentration of Nb thus always showed a comparably high concentration of Co. This effect of so-called 'co-solubility' suggests that both elements preferably enter the perovskite lattice as the complex $[Nb^{5+}_{2/3}Co^{2+}_{1/3}]^{4+}$, rather than as separate $[Nb^{5+}]^{\cdot}$-donors or $[Co^{2+}]^{''}$-acceptors. Most probably, the complex perovskite $Ba(Co_{1/3}Nb_{2/3})O_3$, reported by Galasso[15] strongly modifies the Curie point of $BaTiO_3$. Hence, the Co_3O_4 additive not only regulates diffusion and incorporation of Nb_2O_5 but

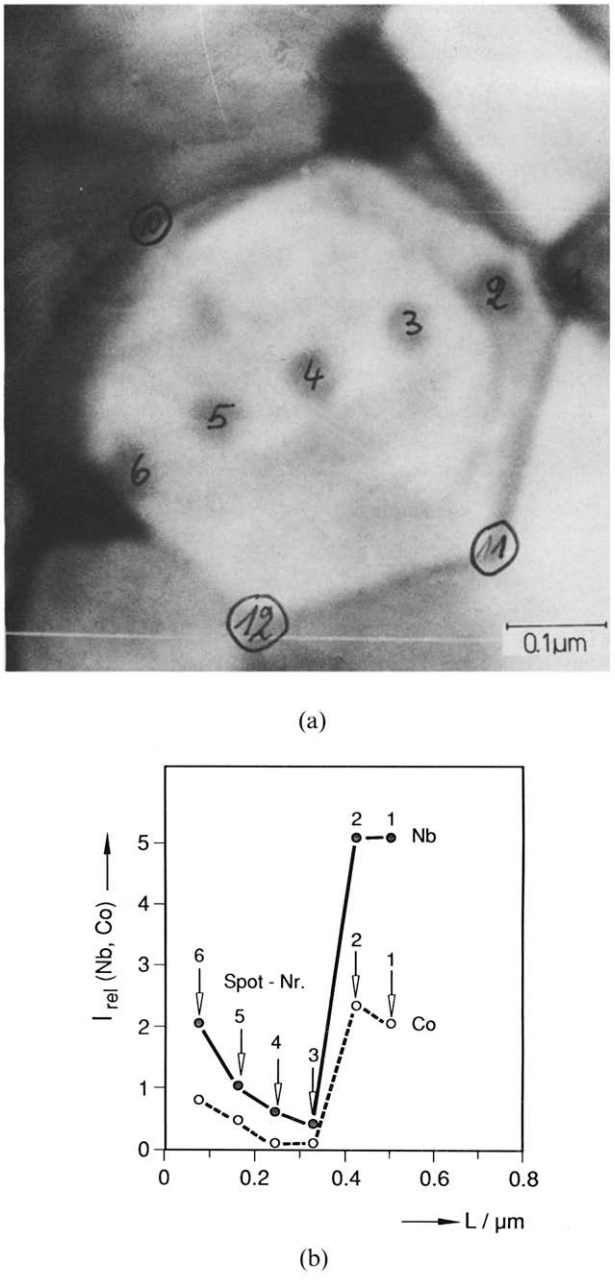

Fig. 8. STEM–EDAX microspot analysis of Co and Nb along a line through a core-shell grain of $BaTiO_3$–Nb_2O_5–Co_3O_4 material. (a) STEM micrograph of analyzed grain; (b) analysis of Nb and Co-concentration in arbitrary units, corresponding to count rates of Nb- and Co-K_α.

also decisively influences the temperature characteristic of the dielectric material.

3.3.2 Nb-mapping in X7R capacitors

Nb mapping of industrial X7R ceramics occasionally reveals larger regions of almost pure $BaTiO_3$. Such irregularities of the microdistribution of Nb and Co usually extend over dimensions of 2–3 µm. The irregularities are assumed to result from particle aggregates in the $BaTiO_3$ powder. Figure 9(a) shows the Nb mapping of a X7R material, containing such 'flakes' of undoped $BaTiO_3$.

In undoped $BaTiO_3$ the number of ionized oxygen vacancies[21] is significantly higher than in

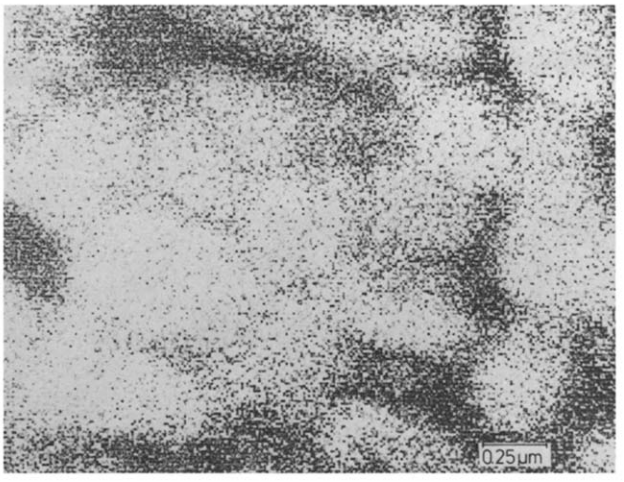

(a)

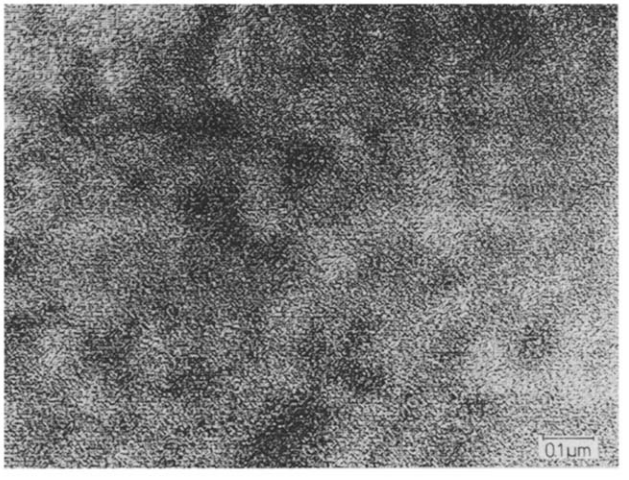

(b)

Fig. 9. STEM–EDAX Nb-K_α mapping of $BaTiO_3$–Nb_2O_5/Co_3O_4 X7R material, fired 2 h at 1300°C: (a) aggregated powder, (b) with hydrothermal $BaTiO_3$ powder.

donor-doped material. Electromigration[22] of ionized oxygen vacancies, $[V(o)]^{\cdot\cdot}$, through the flakes possibly gives rise to rapid electrical degradation and breakdown. A detailed interpretation of the effects of electromigration of charged oxygen vacancies is given by Waser and coworkers.[22,23]

From a statistical point of view, some of the flakes are expected to touch each other, thus forming larger clusters of undoped $BaTiO_3$. In thin dielectric layers such clusters of undoped $BaTiO_3$ may extend from one electrode to the other. Hence, the thickness of the dielectric layers lies within the 'percolation limit' of the lower insulating $BaTiO_3$ flakes.

Mixtures of monodispersed, hydrothermal $BaTiO_3$ with fine-grained Nb_2O_5 and Co_3O_4 exhibit a much finer degree of heterogeneity. As can be seen from Nb-mapping (Fig. 9(b)) no $BaTiO_3$ flakes appear in ceramics of hydrothermal $BaTiO_3$. In spite of the very fine distribution of Nb and Co, these materials display the typical, flat X7R characteristic.

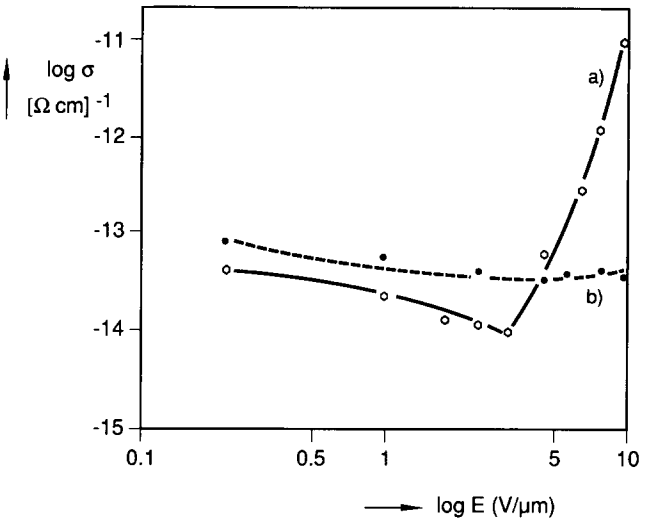

Fig. 10. Specific conductivity of 200 μm discs of $BaTiO_3$–Nb_2O_5/Co_3O_4, fired 2 h at 1300°C, measured as function of the DC field (V/μm) at 125°C: (a) conventionally mixed BTO-based $BaTiO_3$ powder, (b) hydrothermal $BaTiO_3$ powder.

3.4 Improved dielectric materials

X7R materials prepared from hydrothermal $BaTiO_3$ showed an improved dielectric strength, as compared to those prepared from conventional, aggregated $BaTiO_3$ powders. Figure 10 shows the field dependence of the specific resistance σ of two 200-μm thick disc capacitors. The capacitors had the same nominal composition but were prepared from different $BaTiO_3$ powders. At $E < 5$ V/μm the conductivity σ of both materials was almost independent of the DC field applied. At DC fields $E > 5$ V/μm the conductivity of the sample made from conventional aggregated $BaTiO_3$ became strongly field dependent, while that of materials produced from hydrothermal $BaTiO_3$ remained unchanged up to very high fields.

4 Discussion and Conclusions

Microheterogeneity is considered to be the fundamental prerequisite for temperature stability of $BaTiO_3$-based X7R dielectrics. In ceramics of the system $BaTiO_3$–Nb_2O_5–Co_3O_4 a high degree of chemical heterogeneity was observed inside the grains. At the reaction of Nb_2O_5 and Co_3O_4 with $BaTiO_3$ various intermediate phases are rapidly formed. Diffusion of Nb and Co from these intermediate phases into the perovskite lattice of $BaTiO_3$ is very slow. The transport of Nb and Co is promoted by molten eutectic phases in the system $BaTiO_3$–TiO_2. The Co_3O_4 additive shows a pronounced co-solubility with Nb_2O_5. Nb^{5+}-donors are compensated by Co^{2+}-acceptors on Ti sites. The complex $[Nb_{2/3}Co_{1/3}]^{4+}$ substituting for Ti^{4+} largely determines the dielectric temperature characteristic of the material.

In thin dielectric layers of $BaTiO_3$–Nb, Co X7R materials the dielectric strength and life stability is determined by the interconnection of undoped $BaTiO_3$ microregions, showing a lower insulation resistance. The percolation limit of the undoped $BaTiO_3$ regions depends critically on the micro-heterogeneous distribution of Nb_2O_5 and Co_3O_4 over the $BaTiO_3$.

Acknowledgements

The authors are greatly indebted to B. Schmidl for tape-casting of $BaTiO_3$ and Nb_2O_5, K. Herff for preparing light micrographs, B. Krafczyk for SEM, G. Rosenstein for TEM investigation and S. Hûnten for electrical measurements.

References

1. Hennings, D., Barium titanate based ceramic materials for dielectric use. *Int. J. High Tech. Ceram.* **3** (1987) 91–111.
2. Rawal, B. S., Kahn, M. & Buessem, W. R., Grain core-grain shell structures in barium titanate-based dielectrics. In *Advances in Ceramics*, Vol. 1. American Ceramic Society, Columbus, OH, 1981, pp. 172–88.
3. Hennings, D. & Rosenstein, G., Temperature-stable dielectrics, based on chemically inhomogeneous $BaTiO_3$. *J. Am. Ceram. Soc.* **67** (1984) 249–54.
4. Arlt, G., Hennings, D. & DeWith, G., Dielectric properties of fine-grained barium titanate. *J. Appl. Phys.*, **58** (1985) 1619–25.
5. Jonker, G. H. & Noorlander, W., Grain size of sintered barium titanate. In *Science of Ceramics I*, ed. G. H. Stewart. Academic Press, London, 1962, p. 255.
6. Subbarao, E. C. & Shirane, G., Dielectric and structural studies in the system $Ba(Ti,Nb)O_3$. *J. Am. Ceram. Soc.*, **42** (1959) 279.
7. Kahn, W. R. & Buessem, W. R., Effects of grain growth on the distribution of Nb in $BaTiO_3$ ceramics. *J. Am. Ceram. Soc.*, **7** (1971) 458.
8. Burn, I., Temperature-stable barium titanate ceramics containing niobium pentoxide. *Electrocomponent Sci. Technol.*, **2** (1976) 241–7.
9. Clabaugh, W. S., Swiggard, E. M. & Gilchrist, R., Preparation of barium titanyl oxalate tetrahydrate for conversion to barium titanate of high purity. *J. Res. Natl. Bur. Stand.*, **56** (5) (1956) Res. Paper 2677, 289–91.
10. Hennings, D., Rosenstein, G. & Schreinemacher, H., Hydrothermal preparation of barium titanate from barium-titanium acetate gel precursors. *J. Eur. Ceram. Soc.*, **8** (1991) 107-15.
11. Negas, T., Roth, R. S., Parker, H. S. & Minor, D., Subsolidus phase relations in the $BaTiO_3$–TiO_2 system. *J. Solid State Chem.*, **9** (1974) 297–307.
12. Daniels, J., Härdtl, K. H. & Wernicke, R., The PTC-effect of $BaTiO_3$. *Philips Technische Rundschau*, **38** (1979) 3–11.
13. Jonker, G. H. & Kwestroo, W., The ternary systems BaO–TiO_2–SnO_2 and BaO–TiO_2–ZrO_2. *J. Am. Ceram. Soc.*, **41** (1958) 390–14.
14. Hagemann, H. J. & Hennings, D., Reversibe weight change of acceptor doped $BaTiO_3$. *J. Am. Cem. Soc.*, **64** (1981) 590–4.
15. Galasso, F. S., *Structure, Properties and Preparation of Perovskite-Type Components*. Pergamon Press, London 1969.
16. Millet, J. M., Roth, R. S., Ettlinger, L. D. & Parker, H. S., Phase equilibria and crystal chemistry in the ternary system BaO–TiO_2–Nb_2O_5. *Int. J. Solid State Chem.*, **67** (1987) 259–70
17. Roth, R. S., Ettlinger, L. D. & Parker, H. S., Phase equilibria and crystal chemistry in the ternary system BaO–TiO_2–Nb_2O_5. II. New barium polytitanates with <5 mol% Nb_2O_5. *J. Solid State Chem.*, **68** (1987) 330–9.
18. Roth, R. S., Ritter, J. J., Parker, H. S. & Minor, D. B., Synthesis, stability and crystal chemistry of dibarium pentatitanate. *J. Am. Ceram. Soc.*, **69** (1986) 858–62.
19. X-Ray Powder Diffraction File, Alphabetic Index of Inorganic Phases JCPDS, 160 Park Lane, Swarthmore, PA, USA.
20. Mercey, C., Groult, D. & Raveau, B., Insertion of niobium and tantalum in oxides of the type $A_3M_8O_{21}$. *J. Rev. Chim. Miner.*, **16** (1979) 165–73.
21. Daniels, J., Härdtl, K. H., Hennings, D. & Wernicke, R., Defect chemistry and electrical conductivity of doped barium titanate ceramics. *Philips Research Reports*, **31** (1976) 487–566.
22. Waser, R., Processing of dielectric titanates: aspects of degradation and reliability. In *Ferrolectric Ceramics*. Monte Verita, Birkhäuser Verlag, Basel, 1993, pp. 1273–97.
23. Hennings, D., Klee, M. & Waser, R., Advanced dielectrics: bulk ceramics and thin films. *Adv. Mater.*, **3** (7/8) (1991) 334–40.